Macalester Journal of Physics and Astronomy

Volume 6
Issue 1 *Spring 2018*

Article 3

June 2018

Actinometry of Hydrogen Plasmas

A. M. Cotter
Macalester College, acotter@macalester.edu

James Doyle
doyle@macalester.edu

Actinometry of Hydrogen Plasmas

Abstract

Optical emission spectroscopy (OES) can be used to map the electron energy distribution of hydrogen plasmas. Using actinometry, a type of OES where trace amounts of noble gases are introduced, the effect of discharge power on the electron temperature of hydrogen plasmas was explored. This was done using argon and krypton as actinometers for low pressure hydrogen plasmas. It was determined that the electron temperature decreased with respect to power supplied to the discharge.

Keywords

plasma, hydrogen plasma, plasma temperature

1. INTRODUCTION

Hydrogen plasmas are often used to passivate and modify materials, such as thin films. For example, methane is often highly diluted in hydrogen in the Plasma Enhanced Chemical Vapor Deposition of diamond thin films. Besides applied motivations, studying hydrogen plasmas is useful for modeling of reactive plasmas since it is the simplest kind of molecular plasma. In this work, we aim to understand how various parameters affect the electron temperature of hydrogen plasmas. The principal parameter characterizing the electron energy distribution is the electron temperature (T_e). The electron temperature is a fundamental quantity that initiates all processes occurring in the plasma: dissociation, excitation, and ionization.

Optical emission spectroscopy (OES) data can in principle be used to infer the electron energy distribution of hydrogen plasmas. OES is favorable as a method because it is passive and non-perturbative. This method is not particularly useful with pure hydrogen plasmas under the conditions used in this project, due to the complexity and overlap of molecular lines. Thus, a variation of OES known as actinometry was employed. Actinometry is a specific type of OES in which trace amounts of noble gases are introduced into the hydrogen plasma. An actinometer is an inert gas that does not perturb the hydrogen plasma. Because the actinometers have different, well-defined energy thresholds and cross sections, their emission spectra can be used to probe different regions of the electron energy distribution of the plasma. Noble gases can serve as actinometers because in trace amounts they do not perturb the hydrogen plasma.

In this work we use argon and krypton actinometers to study the electron kinetics of hydrogen plasmas. Our objective is to determine the effect of power delivered to the discharge on the electron energy distribution in the plasma.

2. METHODOLOGY

Hydrogen is flowed into the vacuum chamber at 20.0 standard cubic centimeters per minute (sccm). To maintain a partial pressure of 100 mTorr, the gate valve to the turbo pump that is pumping on the system was throttled. Each actinometer (argon or krypton) was maintained at approximately 2.0 mTorr. The plasma was generated using parallel plate electrodes in a vacuum chamber with a base pressure in the 10^{-7} Torr range. Radio frequency power (13.56 MHz) was applied to the electrodes to create the plasma discharge. A matching network was used to minimize the reflected power, thus maximizing the power delivered to the discharge. The experimental setup is shown below in Figure 1.

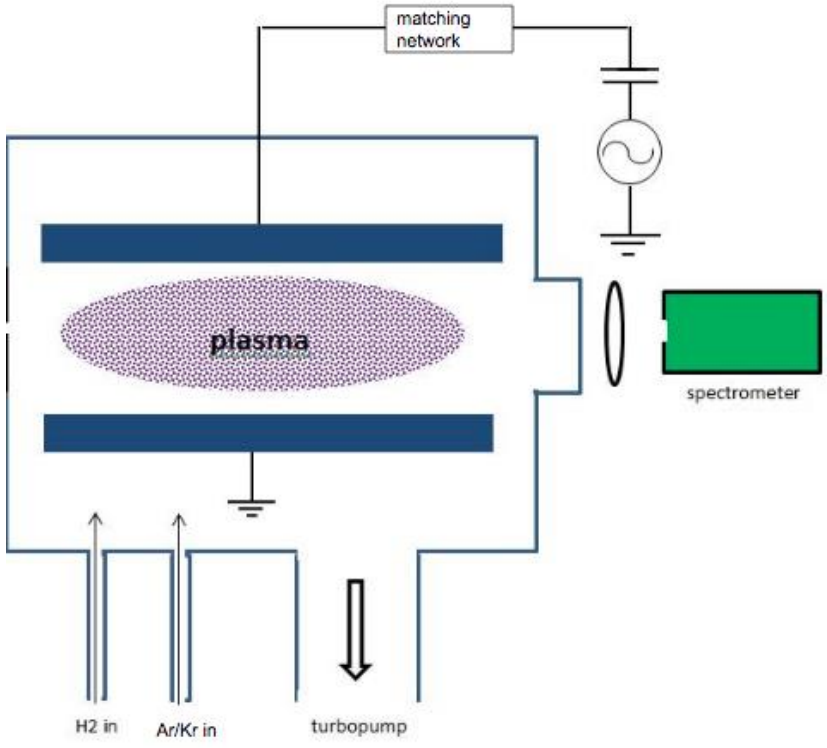

Figure 1. Set-up of vacuum chamber for collection of optical emission data.

Though a matching network is used, it should be noted that the actual power delivered to the discharge was much lower than that of the nominal power since more than 60% of the power delivered by the power supply is dissipated in the network. Each experimental trial consisted of

taking emission spectral data first with hydrogen and the actinometer present, and then removing the actinometer and taking a background (pure hydrogen) spectra. Optical emission data was collected with an Ocean Optics Spectrometer 3000.

Two actinometers are used to probe different energy regions of the electron temperature. Argon and krypton have different lines in their spectra with different threshold excitation energies. The range of threshold energies for krypton spectral lines is lower than that for argon spectral lines, as shown by table 1 in the appendix.

Data was taken at six different powers with each actinometer, ranging from 5 to 30 W of nominal power (i.e. without correction of power loss in the matching network). The data collected was used purely for comparative measurements of the change of electron temperature with power and thus absolute power measurements are not required.

3. RESULTS

Krypton and argon spectra were obtained by subtracting the actinometer spectra from the background spectra as described above. Sample spectra are shown in Figures 2 and 3.

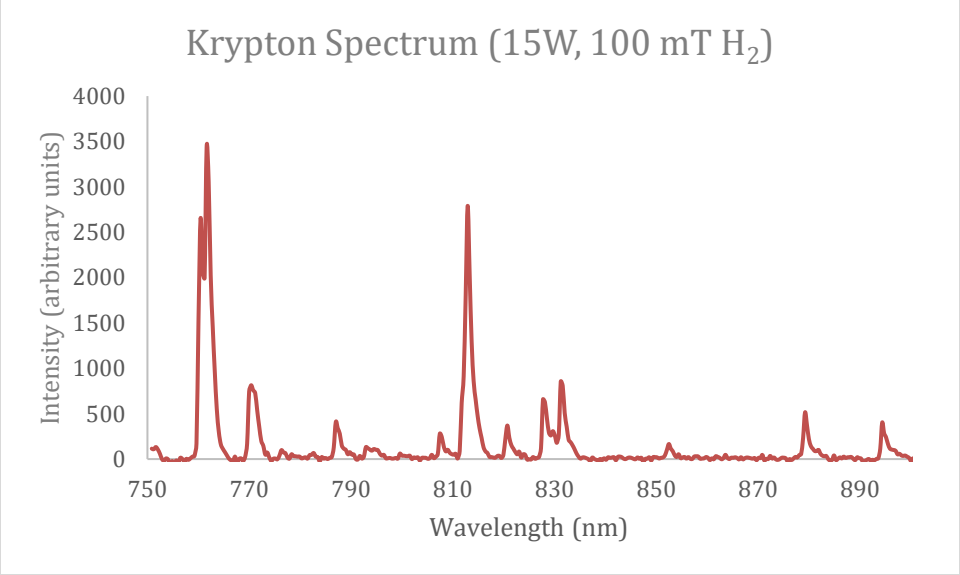

Figure 2. A krypton spectra obtained through the subtractive method from trials at 15 W nominal power and 100 mTorr H_2 as described in the methodology section.

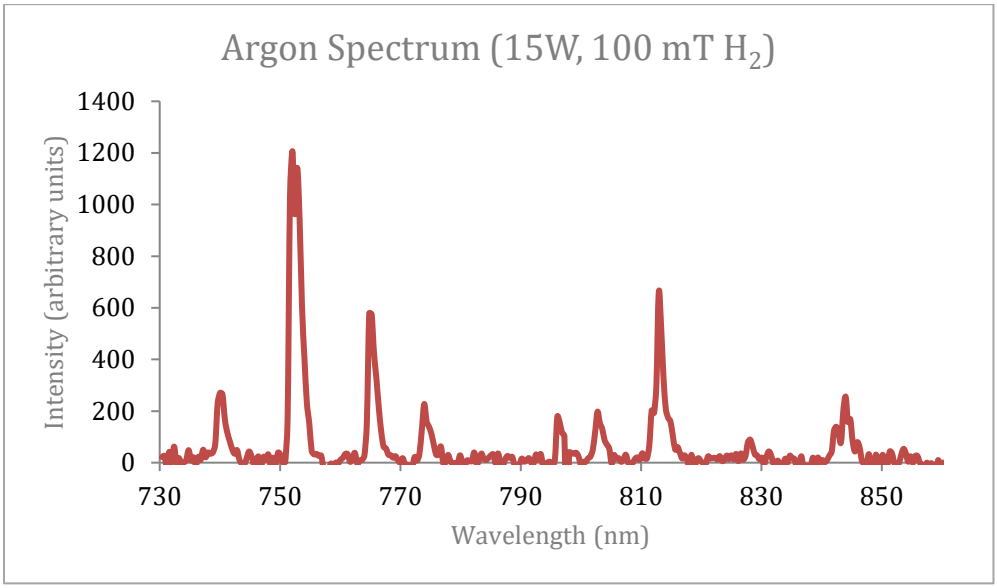

Figure 3. An argon spectra obtained through the subtractive method from trials at 15 W nominal power and 100 mTorr H_2 as described in the methodology section.

As seen in these spectra, certain emission lines could not be fully resolved with the spectrometer used. Seven distinct krypton emission lines and five distinct argon emission lines were selected for comparative analysis. The intensities of each of the krypton peaks were then normalized to the intensities of the five argon peaks and then plotted with respect to nominal power. From this data, a final normalization occurred: each data set was normalized to the emission line ratio intensity value occurring at the lowest power so that any trend in the emission data would be easily observed. As seen in Figures 4-8, the ratio (Kr/Ar) increases with respect to increasing nominal power. This trend is consistent across all the emission data.

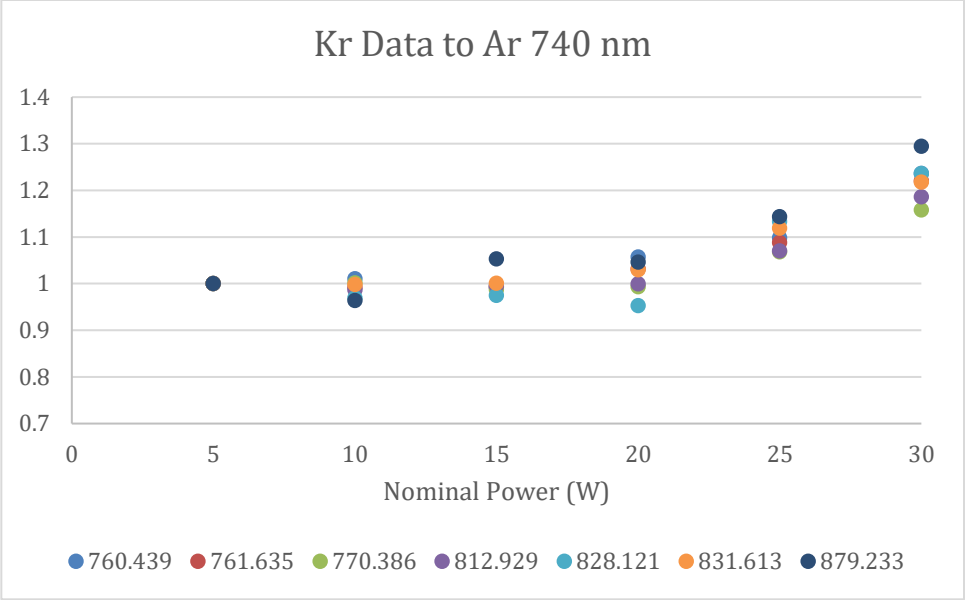

Figure 4. Krypton emission data of six emission lines (as noted in the legend) normalized to the argon 740 nm emission line at nominal powers ranging from 5-30W.

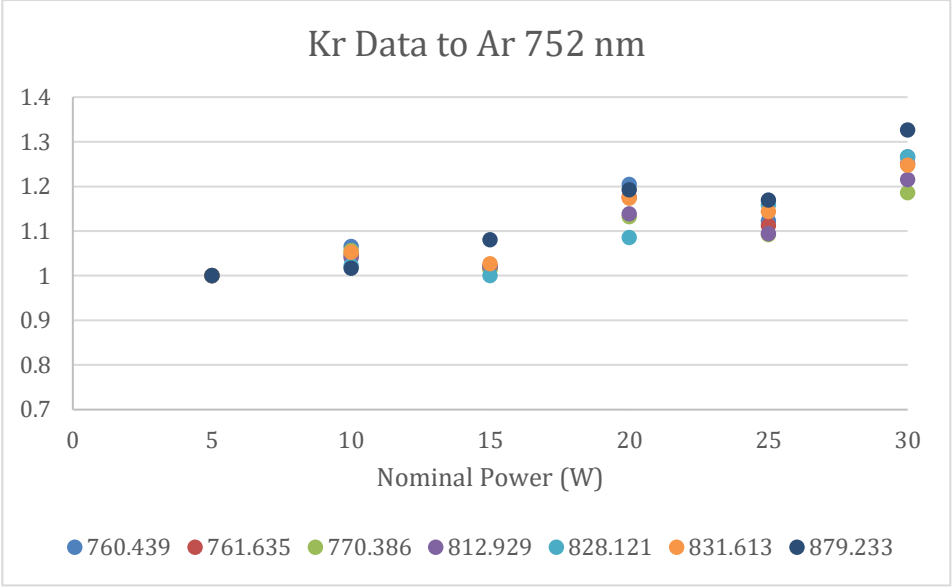

Figure 5. Krypton emission data of six emission lines (as noted in the legend) normalized to the argon 752 nm emission line at nominal powers ranging from 5-30W.

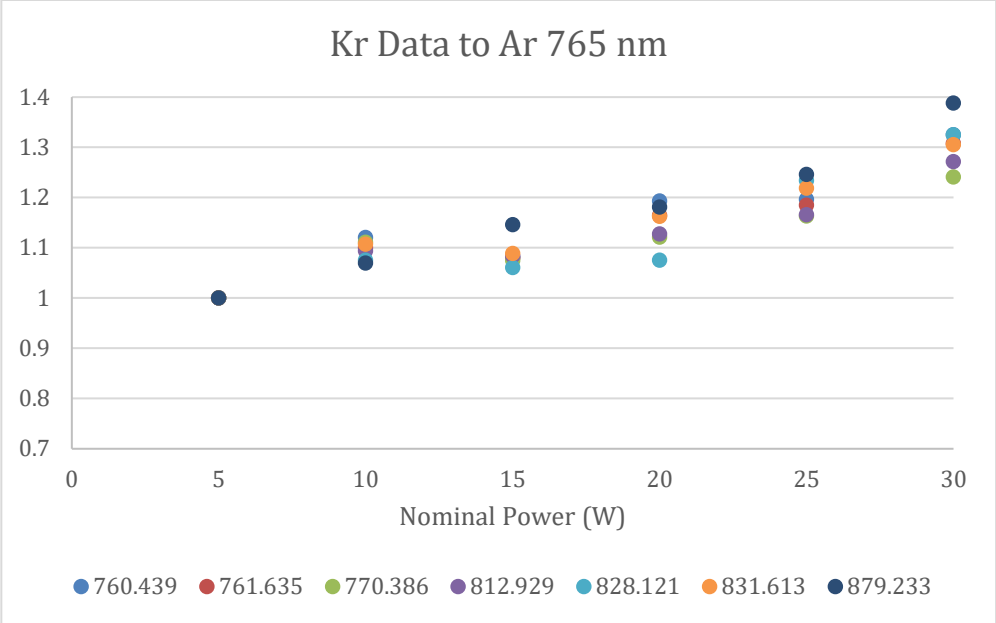

Figure 6. Krypton emission data of six emission lines (as noted in the legend) normalized to the argon 765 nm emission line at nominal powers ranging from 5-30W.

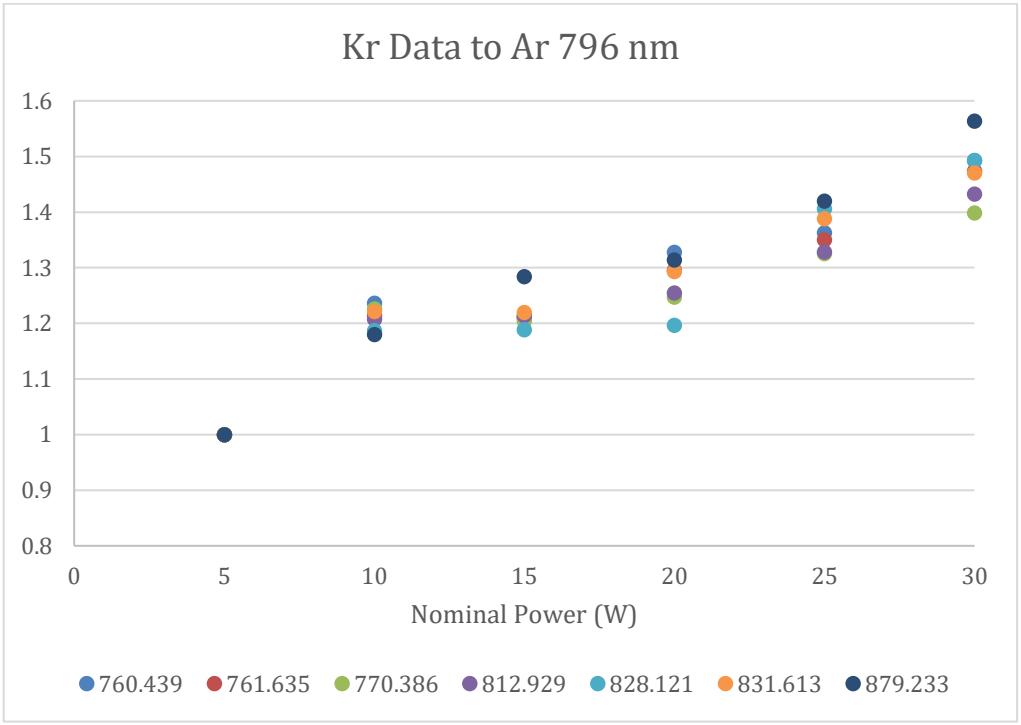

Figure 7. Krypton emission data of six emission lines (as noted in the legend) normalized to the argon 796 nm emission line at nominal powers ranging from 5-30W.

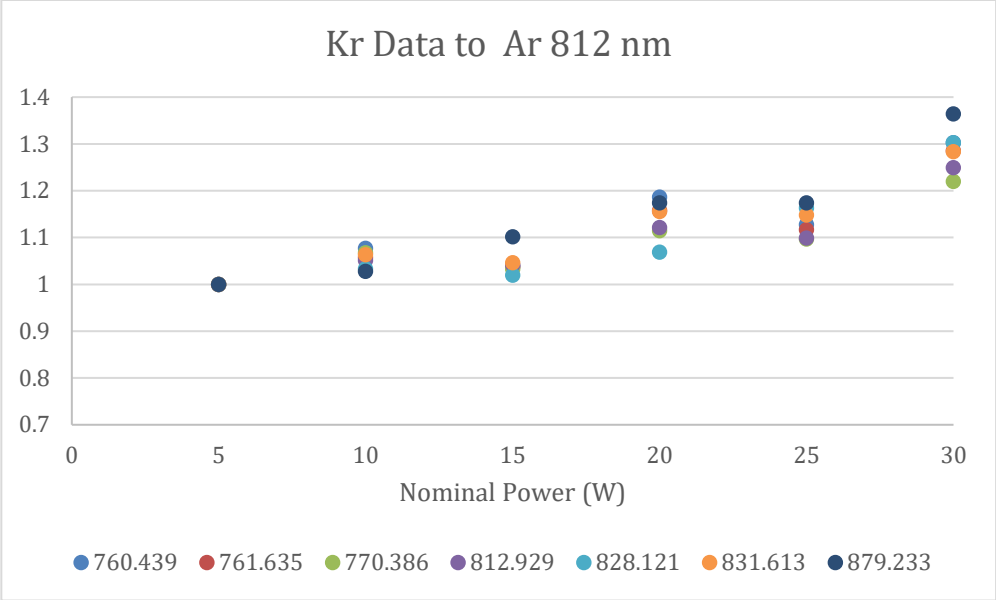

Figure 8. Krypton emission data of six emission lines (as noted in the legend) normalized to the argon 812 nm emission line at nominal powers ranging from 5-30W.

4. DISCUSSION

4.1. Qualitative Model

A key assumption within our work is that the electron energy distribution can be mapped with a Boltzmann distribution so that the single parameter of electron temperature can be used to characterize the distribution. This assumption is fairly common in fundamental studies of hydrogen plasmas. However, it is a simplification and deviations can occur, particularly the existence of a high energy tail.

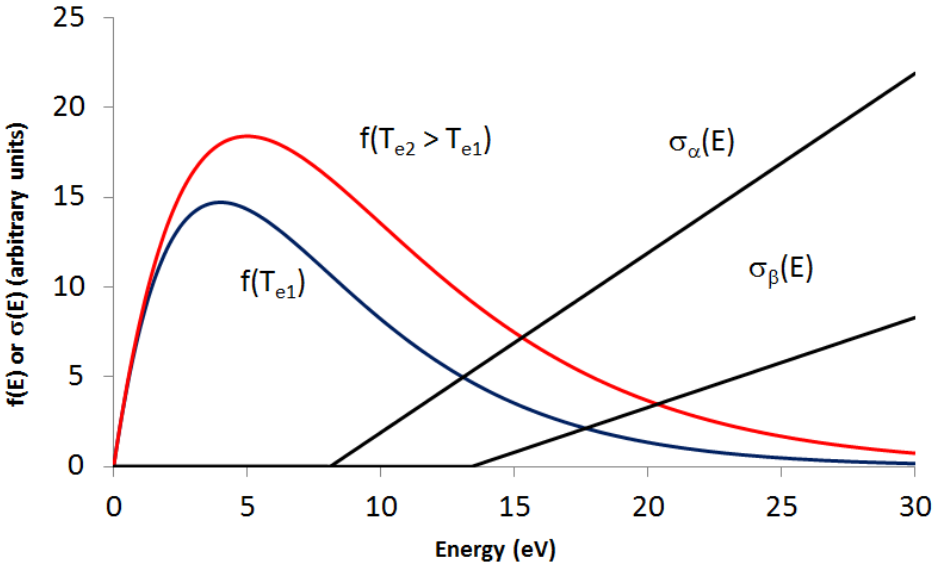

Figure 9. A plot of two Maxwellian electron temperatures shown in red and blue as compared to two cross sections of different excitation thresholds. In this Figure, σ_α represents the krypton excitation cross section, and σ_β represents the argon cross section.

Assuming the electron distribution is Maxwellian, the qualitative behavior of the actinometry results can be understood using a simple model for the krypton and argon electron collisional excitation cross sections Using this model, we can calculate the ratio of expected emission intensities for the argon lines versus the krypton lines as a function of electron temperature. The difference in excitation thresholds allows insight into how the electron temperature changes as a result of changing the amount of power delivered to the discharge. In other words, if we were to take a ratio of emission data of at least one emission line with each actinometer, comparing these ratios across powers allows us to make at least qualitative statements about how the electron temperature changes. Figure 9 shows that the ratio of a krypton emission line to an argon emission line would decrease with respect to nominal power if the electron temperature were increasing, and decrease if the electron temperature were increasing. Such a qualitative model provides the foundation for the quantitative model in the following section.

4.2. Quantitative Model

The quantitative model can be used to compare the ratio of krypton emission to argon emission for various spectral peaks. The calculation is a convolution of the electron energy distribution of the plasma and the cross sections of the actinometers.

$$\rho \equiv \frac{Kr}{Ar} = \frac{\int f(E) E\, \sigma_{Kr}(E)\, dE}{\int f(E) E\, \sigma_{Ar}(E)\, dE} \quad (1)$$

in which:

$$f(E) = E\, e^{\frac{-E}{T_e}} \quad (2)$$

One prominent peak respectively from the argon and krypton spectra were selected for this model. Information regarding cross sections and energy excitation thresholds obtained from M. Malyshev and V. Donnelly can be found in table I in the appendix (1997). A sample range of data of electron temperatures ranging from 3-5 eV is plotted in Figure 10. This range of electron temperatures was selected because it would be expected to be experimentally observed for hydrogen plasmas occurring under the conditions used in this experimental work.

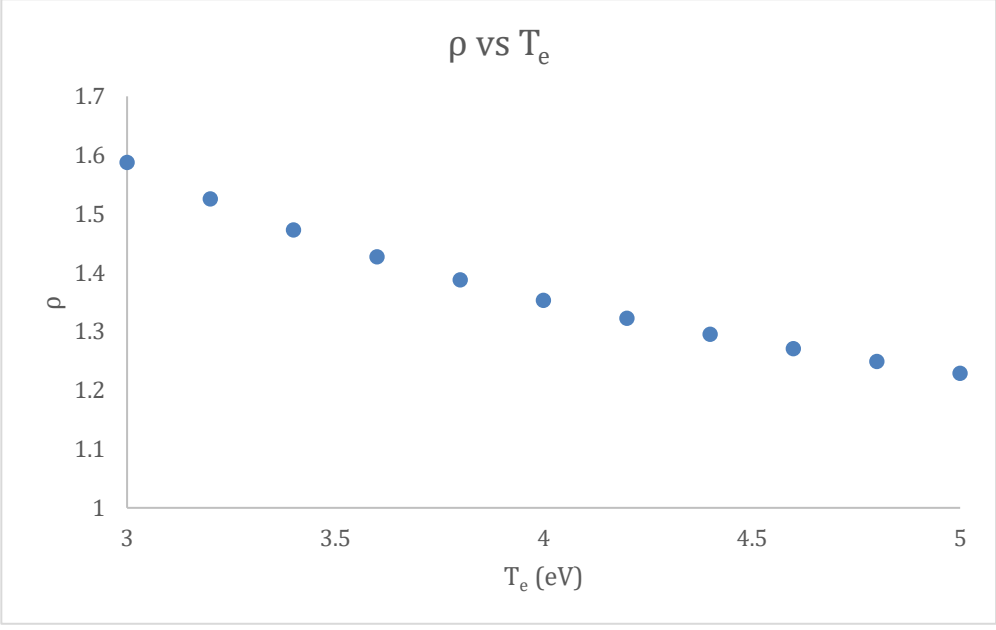

Figure 10. A plot ρ versus the electron temperature (T_e) of the hydrogen plasma.

From this plot, we observe that ρdecreases with respect to increasing electron temperature. As seen in figures 4-8, ρ is experimentally observed to increase with respect to power. Thus, it is concluded that the electron temperature is decreasing with respect to power. This is most likely due to an increased electron density in the plasma with greater power supplied to the discharge.

4.3. Model Limitations

The model described above does not allow for accurate estimates of the electron temperature since it does not account for other types of emission from the plasma. We assume the primary channel of reactions resulting in emission are direct excitations.:

$$e^- + Ar \rightarrow Ar^* + e^- \rightarrow Ar + e^- + \lambda \quad (3)$$

$$e^- + Kr \rightarrow Kr^* + e^- \rightarrow Kr + e^- + \lambda \quad (4)$$

However, our model does not take into account any cascading effects, that is, emission from a state that is populated by decay from higher states rather than direct excitation. Nonetheless, the qualitative conclusion that the electron temperature is decreasing with increasing power is robust, since this result is due only to the fact that the krypton excitations have a lower excitation threshold than the argon excitations.

From our simple quantitative model, we can conclude that the electron temperature decreases with respect to increasing nominal power. This is most likely due to the fact that as power to the discharge is increased, the plasma density of the plasma also increases. Higher plasma density then leads to an increased number of electron-ion collisions which should result in a decrease in electron energy on average.

The electron temperature of the hydrogen plasma could in principle be estimated from this data. Such an analysis, however, requires a complicated mathematical model that would account for cascading effects. This is an objective in future work of the fundamental study of hydrogen plasmas.

The author would like to thank James Doyle for his guidance in this work and Ken Moffett for technical assistance. Support for this work was provided by the Beltmann Fund.

5. REFERENCES

A. Cotter, A. Stowell, J. Carlson, and J.R. Doyle, Journal of Vacuum Science & Technology A: Vacuum, Surfaces, and Films **36**, 031304 (2018).

V.M. Donnelly, Journal of Physics D: Applied Physics **37**, (2004).

C. Karolis and E. Harting, Journal of Physics B: Atomic and Molecular Physics **11**, 357 (1978).

M.V. Malyshev and V.M. Donnelly, Journal of Vacuum Science & Technology A: Vacuum, Surfaces, and Films **15**, 550 (1997).

M.V. Malyshev and V.M. Donnelly, Physical Review E **60**, 6016 (1999).

L. Marques, J. Jolly, and L.L. Alves, Journal of Applied Physics **102**, 063305 (2007).

S. Siepa, S. Danko, T.V. Tsankov, T. Mussenbrock, and U. Czarnetzki, Journal of Physics D: Applied Physics **47**, 445201 (2014).

6. APPENDIX

Gas	Wavelength (nm)	Exp. Wavelength (nm)	Energy Threshold (eV)
Argon	750.4	751.6	13.5
	751.5	752.4	13.3
	763.5	764.8	13.2
	794.8	796	*
	811.5	812.5	13.1
Krypton	758.7	760	11.7
	760.2	761.2	11.5
	768.5	769.5	12.2
	769.5	769.9	11.5
	810.4	811.3	11.4
	811.3	812.5	11.4
	826.3	827.3	12.2
	829.8	830.8	11.5
	877.7	878.8	11.4

Table I. Argon and krypton spectral line wavelengths as recorded in Malyshev and Donnelly's article on actinometry (1997) and observed experimentally, tabulated with the corresponding threshold for excitation.